

Exploring Semi-Supervised Learning for Online Mapping

Adam Lilja^{1,2}, Erik Wallin^{1,3}, Junsheng Fu², and Lars Hammarstrand¹

¹Chalmers University of Technology

²Zenseact

³Saab AB

{firstname.lastname}@{zenseact.com, chalmers.se, saabgroup.com}

Abstract—Online mapping is important for scaling autonomous driving beyond well-defined areas. Training a model to produce a local map, including lane markers, road edges, and pedestrian crossings using only onboard sensory information, traditionally requires extensive labelled data, which is difficult and costly to obtain. This paper draws inspiration from semi-supervised learning techniques in other domains, demonstrating their applicability to online mapping. Additionally, we propose a simple yet effective method to exploit inherent attributes of online mapping to further enhance performance by fusing the teacher’s pseudo-labels from multiple samples. The performance gap to using all labels is reduced from 29.6 to 3.4 mIoU on Argoverse, and from 12 to 3.4 mIoU on NuScenes utilising only 10% of the labelled data. We also demonstrate strong performance in extrapolating to new cities outside those in the training data. Specifically, for challenging nuScenes, adapting from Boston to Singapore, performance increases by 6.6 mIoU when unlabelled data from Singapore is included in training.

I. INTRODUCTION

An autonomous vehicle needs to understand where it is safe to drive. This includes knowing where other road participants are and where the lane delimiters and road edges are located around the vehicle. Relying solely on pre-made offline High-Definition (HD) maps for road information comes with difficulties, such as accurate localisation within the map, and the costs associated with building and keeping the maps up to date. The latter is significant for scaling Autonomous Driving (AD) beyond limited, well-defined areas. Online mapping is an alternative and complementary approach, where onboard sensory data is used to produce a local up-to-date map depicting surrounding lane markers, road edges, and pedestrian crossings in real-time [24, 25].

Recent studies have shown that end-to-end learning-based online mapping algorithms struggle to generalise to regions not present in their training set, suggesting that the available data is insufficient for learning this complex task [27, 29]. While collecting large amounts of AD data is relatively straightforward, the bottleneck lies in the effort needed to label the data. Creating the necessary labels, *e.g.* 3D polylines for each lane divider, is generally time-consuming and costly. Therefore, we are interested in approaches that utilize a small amount of labelled data and a vast amount of unlabelled data to increase the generalisability in the online mapping task.

Other domains, such as image classification [39] and semantic segmentation [13], have addressed this problem setting through Semi-Supervised Learning (SSL) and shown remarkable capabilities. Recently the interest in SSL for object detection has also gained traction and shown promising

results [32, 47]. Some SSL techniques have also been successfully adapted to the closely related domain of Bird’s Eye View (BEV) semantic segmentation. For instance, utilising a teacher-student setup [39] has demonstrated effectiveness in monocular BEV segmentation, applicable to both dynamic classes such as vehicles and pedestrians, and static classes including drivable areas, and walkways [55, 14]. However, new challenges arise when multiple cameras are used as input, as creating 3D-consistent augmentations in this context proves difficult. For instance, the conjoint-rotation technique introduced by Zhu et al. [55] is incompatible with our problem setup. Concurrent work has shown that randomly disabling entire camera feeds and applying dropout on the BEV features as strong augmentation for the student are effective when surround-view images are used as input [21].

In this work, we aim to identify which key SSL approaches excel in the online mapping domain and explore how to best leverage the unique characteristics of online mapping. For instance, the static nature of objects in online mapping allows for leveraging temporal consistency to enhance performance, which is not possible in the more general problem formulation of BEV semantic segmentation. In this spirit, we propose and investigate a label-efficient SSL method, illustrated in Fig. 1, that uses sequential data to enable the teacher to fuse information across multiple samples and thus produce more reliable pseudo-labels. This approach effectively boosts performance in online mapping leveraging less expensive unlabelled data.

This paper makes four key contributions: First, we conduct a comprehensive analysis of prevalent SSL techniques for online mapping, demonstrating which existing methods can significantly enhance performance. Second, we propose using the static-world assumption to improve pseudo-label accuracy by enabling the teacher model to integrate information across multiple samples. Third, we combine SSL components into a robust method that maintains high performance levels across varying volumes of labelled data. Lastly, we demonstrate this method’s additional benefit of strong performance in domain adaptation when trained in one group of cities and evaluated in another.

II. RELATED WORK

This work explores which semi-supervised learning, and domain adaptation, approaches excel when applied to the online mapping setting. Thus, we describe these fields in the following section.

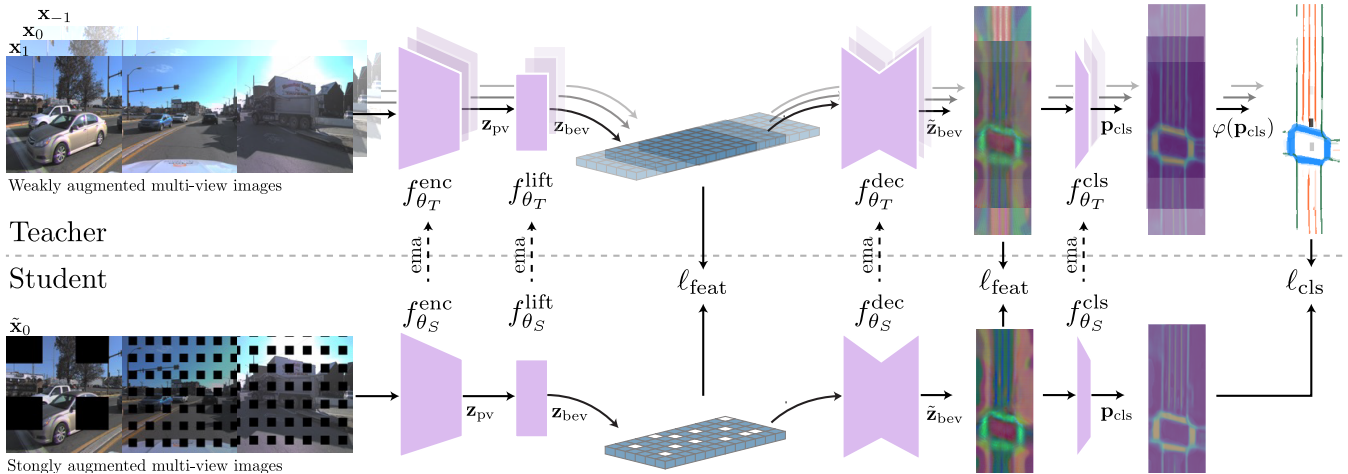


Fig. 1: Self-training with Teacher Student set-up for Online Mapping.

A. Semi-Supervised Learning

In SSL, we combine costly labelled data with inexpensive unlabelled data to train a model. There are two main approaches to this problem, single-stage training where automatic ground truth labels are generated during training, *i.e.* using predictions from a single model or an ensemble of models as pseudo-labels [37, 51, 23], or a two-stage process starting with self-supervised pre-training followed by finetuning on the labelled data [8, 19, 5]. This paper concentrates on the single-stage joint training approach, exploring critical design decisions and their impact on the performance of semi-supervised online mapping.

SSL has a rich history in image classification, with the teacher-student framework [39] being particularly influential. This framework involves a student network supervised by predictions from a teacher network. The teacher network shares the same architecture as the student but updates its weights as an exponential moving average (EMA) of the student’s weights. ReMixMatch [1] further introduced the idea of feeding the teacher model weakly augmented inputs, while the student model receives strongly augmented inputs. Many works have highlighted the importance of data augmentation in SSL [54, 13, 41] and these augmentations may differ from those suitable for fully supervised settings [54]. Common augmentation strategies for SSL include RandAugment [10], CutOut [11], CutMix [49], and feature dropout [48].

FixMatch [37] further popularized *thresholding*, a technique where the student is supervised only with high-confidence pseudo-labels generated by the teacher. Numerous follow-up studies continue to demonstrate the strengths of this method [48, 44]. Another line of work in SSL involves adding self-supervised auxiliary tasks to improve performance, such as predicting the parameters of stochastic image transformations applied to unlabelled images [43, 50] or adding similarity loss of the features between the teacher and student models [9, 42].

Research in SSL has also been extended to BEV segmentation, considering a variety of classes such as car, truck, road, walkway, and vegetation [14, 55, 15, 16]. The teacher-student approach has, for instance, been adapted to monocular BEV

segmentation, utilizing MSE losses for probability and feature similarity [55, 14]. Unlike in Perspective View (PV) semantic segmentation, where a variety of augmentations are permissible, the augmentations applied in BEV segmentation must maintain 3D consistency. *E.g.*, methods such as randomly cropping and resizing the PV input image for BEV segmentation can break geometric consistency in the BEV plane. One augmentation with geometric consistency is the conjoint rotation introduced in [55] where both images and BEV pseudo-labels are rotated around the upward axis. However, this technique is limited to monocular camera setups, as any augmentation affecting the 3D geometry must maintain 3D consistency across all cameras.

Our setup closely resembles the concurrent work of PCT [21], which proposes SSL on multi-view images using a teacher-student framework inspired by [48]. They introduce a camera dropout augmentation technique, where one or more camera images are omitted for the student model, and leverage BEV feature dropout. Additionally, they use pre-trained models to generate PV semantic segmentation and depth pseudo-labels. However, in this paper, we focus on core SSL methods without incorporating additional pre-trained networks for pseudo-labeling.

B. Domain Adaptation

Unsupervised domain adaptation (UDA) is a field closely related to SSL, where the unlabelled data is drawn from a target domain that is slightly shifted from the source domain (labelled data). The goal of UDA is to achieve strong performance in the target domain and is of great importance to AD as we want to generalise to new geographical regions. UDA incorporates many techniques commonly used in SSL, with self-training being the most prominent [56]. There are many works on UDA for semantic segmentation with AD applications in mind. The dominant approach in these works involves augmenting data by mixing crops of labelled and unlabelled data [40, 7]. However, such augmentations are not well-suited for our setting, as online mapping requires consistency across multiple camera views.

C. Online Mapping

Recently, significant progress has been made in the field of online mapping, leading to the development of two primary approaches: segmentation-based methods [46, 12, 24, 34] and vector-based methods [31, 25, 26, 6] where the key difference lies in the output representation. Segmentation-based methods rasterize a region from a Bird’s Eye View and classify each cell, typically using a CNN [35, 12, 24]. The vector-based methods predict vectors with connected points, representing a polyline for each object, typically using a DETR-like [4] transformer decoder [25, 26, 53].

Both approaches encode input images using a neural network and transform the features into BEV using a core technique known as *lifting*. For instance, LSS [36] learns a categorical depth distribution for each pixel and use it to weigh how much the corresponding PV feature should influence the corresponding BEV-cell.

We are mainly interested in the effects of SSL approaches and will use a segmentation-based method as the formulation is a better match for existing SSL and UDA methods.

III. SSL FOR ONLINE MAPPING

Our work focuses on leveraging SSL to maximize the effectiveness of unlabelled data in online mapping. In this context, we assume that we have a small set of labelled data $\mathbf{X}_L = \{\mathbf{x}_i, \mathbf{y}_i\}_{i=1}^{n_l}$, for which ground truth map \mathbf{y}_i is available, and a large set of unlabelled images $\mathbf{X}_U = \{\mathbf{x}_i\}_{i=1}^{n_u}$ without ground truth annotations. The latter is assumed to be collected in areas separate from the labelled set, but using the same cameras. Further, the relative pose of the vehicle in the sequences is assumed to be known.

Using the labelled data, the student is trained in an ordinary supervised manner by minimizing a supervised loss $\ell_{\text{sup}}(\mathbf{x}_i, \mathbf{y}_i)$, e.g., cross-entropy, DICE [38], or Focal Loss [28]. Effectively using the unlabelled data is more challenging as we do not have access to a ground truth map for this area, and several design choices must be made. To understand how to apply SSL methods in the context of online mapping, we explore the impact of these choices using a well-established online mapping architecture. Figure 1 shows an overview of the SSL training scheme, and in this section, we provide the details of the online mapping architecture, the prevalent SSL techniques we employed, and our proposed simple multi-step teacher fusion approaches.

A. Online mapping architecture

As we are mainly interested in the effects of SSL approaches, we choose to use a typical map segmentation architecture [24, 52, 34] such as Fig. 1 illustrates. A set of multi-view images, \mathbf{x} , is individually encoded by a neural network $\mathbf{z}_{\text{pv}} = f_{\theta}^{\text{enc}}(\mathbf{x})$ and lifted to BEV features as $\mathbf{z}_{\text{bev}} = f_{\theta}^{\text{lift}}(\mathbf{z}_{\text{pv}})$. Then, another neural network decodes the BEV features $\tilde{\mathbf{z}}_{\text{bev}} = f_{\theta}^{\text{dec}}(\mathbf{z}_{\text{bev}})$. The final class probabilities are predicted through a classification head $\mathbf{p}_{\text{cls}} = f_{\theta}^{\text{cls}}(\tilde{\mathbf{z}}_{\text{bev}})$, where \mathbf{p}_{cls} comprise the independent probability of each map grid cell containing a lane delimiter, road edge, or pedestrian crossing. As such, the online map is treated as a multi-label

semantic segmentation problem. The complete architecture can be described as $\mathbf{p}_{\text{cls}} = F_{\theta}(\mathbf{x})$.

B. Semi-supervised training scheme

The primary training methodology adopted in this work is based on the Mean Teacher framework [39]. As illustrated in Fig. 1, we use two identical network architectures: a teacher-version, parameterized by θ_T , and a student-version, described by θ_S . In this setup, only the student is trained directly from data, \mathbf{X}_L and \mathbf{X}_U . The teacher weights are updated after each training step using an exponentially moving average (EMA) of the student, $\theta_T \leftarrow \alpha\theta_T + (1 - \alpha)\theta_S$, where α is the keep rate.

We investigate two common forms of SSL schemes, pseudo-labelling and consistency regularization through feature similarity. The first follows the approach in [1, 37, 39, 56], where the student is trained using pseudo-labels (pseudo-maps for our setting) predicted by the teacher. The teacher network receives a weakly augmented version of the input images \mathbf{x} (and possibly a set of additional surrounding data samples, Sec. III-F), for which it predicts a pseudo-map $\hat{\mathbf{y}} = \varphi(F_{\theta_T}(\mathbf{x}))$. Here, $\varphi(\cdot)$ is used to decide/design suitable pseudo-labels based on the predicted class probabilities, e.g., thresholding and/or sharpening (see Sec. III-D). The student receives a strongly augmented version of the same sample $\tilde{\mathbf{x}}$ (see Sec. III-C) and is trained to make consistent class predictions with the teacher model through a pseudo-label loss $\ell_{\text{cls}}(F_{\theta_S}(\tilde{\mathbf{x}}), \varphi(F_{\theta_T}(\mathbf{x})))$.

The feature similarity supervision on the other hand enforces consistency between intermediate features for the teacher and student models. More formally, we train the student network to minimize a feature similarity loss $\ell_{\text{feat}}(\mathbf{z}_{\theta_T}(\mathbf{x}), \mathbf{z}_{\theta_S}(\tilde{\mathbf{x}}))$, where \mathbf{z}_{θ_T} and \mathbf{z}_{θ_S} are intermediate features on the same level, e.g. \mathbf{z}_{bev} or $\tilde{\mathbf{z}}_{\text{bev}}$, using teacher and student models, respectively. In contrast to the pseudo-label training, feature similarity is insensitive to errors in teacher predictions as we avoid any label decisions. We only assume that the representation of the same scene should be consistent in both models. The details of this loss are discussed in Sec. III-E.

In sum, the total training loss for the student is

$$\ell = \sum_{\mathbf{x}_i \in \mathbf{X}_L} \ell_{\text{sup}}(\mathbf{x}_i, \mathbf{y}_i) + \sum_{\mathbf{x}_i \in \mathbf{X}_U} \omega_{\text{cls}} \ell_{\text{cls}}(F_{\theta_S}(\tilde{\mathbf{x}}_i), \varphi(F_{\theta_T}(\mathbf{x}_i))) + \omega_{\text{feat}} \ell_{\text{feat}}(\mathbf{z}_{\theta_S}(\tilde{\mathbf{x}}_i), \mathbf{z}_{\theta_T}(\mathbf{x}_i)),$$

where ω_{cls} and ω_{feat} are hyperparameters controlling the relative importance of the respective loss.

C. Augmentations

The strong augmentation techniques used for the input fed to the student are crucial [54]. Thus, we investigate various data augmentation techniques that do not change the geometry of the scene, as discussed in Sec. II-A. The augmentation techniques investigated in this work include photometric augmentation (random adjustments to brightness, contrast, color conversion, saturation, hue, and channel swaps), camera drop augmentation [21], CutOut [11], and BEV feature dropout inspired by [48].

D. Sharpening and thresholding

In SSL, predictions from the teacher are often refined through thresholding and sharpening before being used as pseudo-labels for the student. Thresholding involves keeping only predictions above some confidence level, whereas sharpening scales the predicted distribution to increase the confidence of the pseudo-label. Although there are many variations of thresholding and sharpening, we focus on a few key approaches. For thresholding, we follow FixMatch [37], *i.e.*, keeping only predictions exceeding a fixed confidence threshold. For sharpening, we explore two techniques: (1) *hard* pseudo-labeling where the teacher predictions are reduced to its argmax [37, 22], and (2) temperature sharpening, where the teacher’s predicted logits are rescaled through division by a temperature parameter (denoted T in [17, 2]) before applying sigmoid to get a *soft* pseudo-label.

E. Feature Similarity

In addition to pseudo-labelling, we can also enforce feature similarity at the BEV feature level, *i.e.* adding the term $\omega_{\text{feat}} \ell_{\text{feat}}(\mathbf{z}_{\theta_T}(\mathbf{x}), \mathbf{z}_{\theta_S}(\tilde{\mathbf{x}}))$ to the total loss. This approach requires the student to maintain consistent BEV features with the teacher, which have been shown to improve performance [42]. While DoubleMatch used cosine similarity as the loss function, previous work on BEV segmentation employed Mean Squared Error (MSE) [55, 14]. We are therefore interested in exploring the impact of the chosen loss function on performance. Another design choice involves determining the optimal stage to harmonize the features between the teacher and the student. We identify two potential levels of interest: immediately following the lifting method, \mathbf{z}_{bev} , and just before decoding the class, $\tilde{\mathbf{z}}_{\text{bev}}$. Incorporating the feature similarity loss can potentially destabilize the training process as overemphasizing this loss may lead to a trivial solution.

F. Teacher Fusion

Unlike BEV segmentation, which includes dynamic classes, all classes in online mapping are stationary. Since sensor data is collected in consecutive sequences with known ego vehicle movement, we can improve the teacher’s pseudo-labels by fusing predictions from multiple nearby samples. As Fig. 1 illustrates, predictions from past and future samples can be inferred and transformed into the current frame. By selecting only the most confident teacher predictions from any of the samples we allow the teacher to have a broader view of the nearby map and make more accurate pseudo-labels. This is especially powerful as predictions far from the ego vehicle tend to be less accurate [12]. As an alternative, we can fuse the BEV features across multiple samples by taking the mean of overlapping processed BEV features $\tilde{\mathbf{z}}_{\text{bev}}$.

To maximize overlap between additional samples and the area of the main sample, and to ensure that these additional samples provide new information, we select them from positions at randomly sampled distances relative to the current main frame. This approach mitigates issues associated with time-based sample selection, such as the ego vehicle being stationary—which offers no additional information—or moving at very high speeds, resulting in little overlap.

TABLE I: Performance (mIoU) of various augmentations.

Photom.	Augmentation			Label utilisation	
	CamDrop	CutOut	BEVDrop	2.5%	10%
✓				12.1±0.6	21.3±0.2
✓	✓			13.3±0.6	32.0±0.1
✓		✓		21.9±1.0	31.9±0.1
✓		✓	✓	24.4±1.2	33.9±0.2
✓		✓	✓	25.5±0.7	34.3±0.1

IV. EXPERIMENTS

To maximize the effectiveness of adding unlabelled data in the online mapping setting, we optimize parameters and design choices for each of the discussed methods and assess the relative impact of different components through ablation studies. Additionally, we examine the usefulness of our method by training on one set of cities and evaluating on another, assessing its capability for domain adaptation.

A. Experimental Setup

We employ a ResNet50 [20] as image encoder f_{θ}^{enc} , LSS [36] for lifting features to BEV f_{θ}^{lift} , and a lightweight convolutional bottleneck decoder inspired by [18] as f_{θ}^{dec} . We perform multi-label prediction for pedestrian crossings, lane dividers, and road boundaries and use Focal Loss [28] as the supervised loss ℓ_{sup} on the labelled dataset and ℓ_{cls} for the unlabelled data. The region of interest follows [30] spanning $\pm 45\text{m}$ longitudinally and $\pm 15\text{m}$ laterally. Each cell has a side length of 0.3m. For brevity, we report the mean Intersection over Union (mIoU) across these three classes. To account for the stochasticity in the results from individual runs, we either report the mean and standard deviation of the mIoU for three runs with the same hyperparameters or multiple nearby values of the hyperparameter. Empirically, we note that our setup is robust to a range of unlabelled weights ω_{cls} spanning 0.25 to 5.0. We choose to follow [14] and use $\omega_{\text{cls}} = 1$. We further follow [21] and linearly ramp-up ω_{cls} , and when applicable ω_{feat} , over the first third of the training. Unless stated otherwise, no thresholding or sharpening is used in the experiments. The models, unless stated otherwise, are trained and evaluated using the Argoverse 2 (AV2) dataset [45] with the geographically disjoint splits proposed by [27] using surround-view camera images as input and use the provided HD maps as labels. We generally experiment using two utilisation rates of labelled data, namely 2.5% and 10%, corresponding to 18 and 70 labelled sequences respectively.

B. Augmentations

Empirically we observe that using a high probability of applying the augmentation yields better performance and choose always to apply the strong augmentations to the student. For the CutOut augmentation, we find that removing 25% of the image yields good results and is thus used for all experiments. For BEV feature dropout (BEVDrop) we follow [21, 48] and drop 50% of the features. The results in Tab. I demonstrate that increasing the difficulty of the task for the student model is crucial also for online mapping. With 10% label utilisation, Photometric augmentation alone is sufficient for significant model improvement. However, with 2.5%

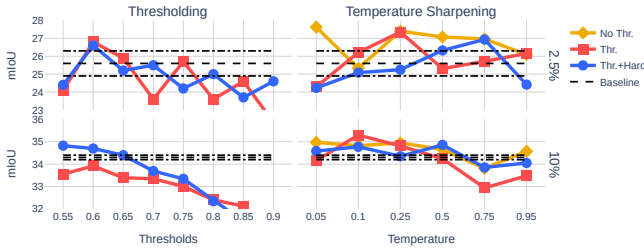


Fig. 2: Thresholding and sharpening utilising 2.5% and 10% of the labels. *Baseline* refers to using only strong augmentations.

TABLE II: mIoU for sharpening methods using threshold 0.6.

Technique		Label utilisation	
Thr.	Hard	2.5%	10%
		25.5 ± 0.7	34.3 ± 0.1
✓		25.1 ± 1.3	33.9 ± 0.1
✓	✓	25.4 ± 0.8	34.6 ± 0.1

label utilisation, additional augmentations are required. For both label utilisation ratios, applying Photometric, CutOut, and BEVDrop yields the best performance, and we adopt this configuration as the *Baseline* in further experiments. Specifically, we observe a significant performance improvement, with mIoU increasing from 12.1 to 25.5 for the 2.5% label utilisation and 21.3 to 34.3 for the 10% label utilization. Furthermore, contrary to the findings in [21], we find that removing parts of the images, *i.e.* CutOut, yields better performance than dropping an entire camera and masking its field of view in the loss, as done with CamDrop.

C. Sharpening and Thresholding

Fig. 2 illustrates the effects of sharpening and thresholding. As shown on the left, supervising with only the most confident pseudo-labels does not yield any additional performance boost. Using a low threshold can marginally improve performance, and we opt to use 0.6 as the threshold in further experiments. Tab. II displays the results over multiple runs using hard and soft labels. We note that there is no significant change in performance using sharpening, which differs from other domains where sharpening has shown to be very effective, usually with high thresholds [37, 48, 44]. While applying sharpening with a temperature parameter can improve performance, right column in Fig. 2, the gains are marginal and introduce an additional hyperparameter.

D. Feature Consistency

We compare the performance using Mean Squared Error (MSE) and Cosine Similarity (COS) losses with $\omega_{cls} = 1$ and varying feature loss weight ω_{feat} . In Fig. 3 the results are displayed using features from before (Pre) or after (Post) the BEV decoder f_{θ}^{dec} as inputs to ℓ_{feat} . When utilizing 2.5% of the labels the results are noisy, and no clear benefit from the additional supervision is observed across the setups. However, for the 10% label utilisation, COS consistency provides a slight performance gain and demonstrates greater stability than the MSE loss. While prior BEV segmentation works opted to use MSE [55, 14], we believe COS to be the better choice.

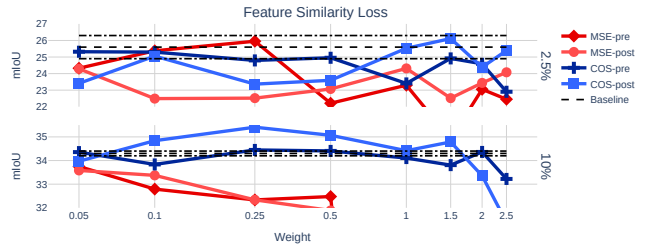


Fig. 3: Feature Similarity using Mean Square Error and Cosine Similarity with varying weights. *Baseline* refers to using only strong augmentations. Pre and Post refers to using \mathbf{z}_{bev} or $\tilde{\mathbf{z}}_{bev}$ respectively.

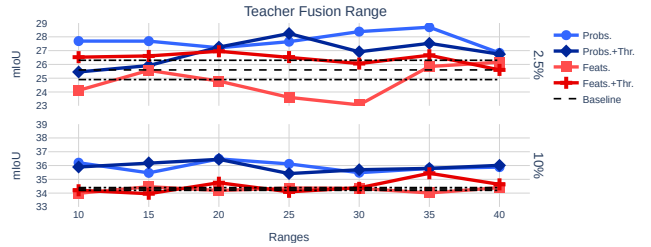


Fig. 4: Teacher Fusion across varying maximum ranges from the current sample. *Baseline* refers using only strong augmentations.

E. Teacher Fusion

To enhance pseudo-labels, we fuse teacher predictions from multiple samples. We use two additional samples, as we empirically found that adding more samples does not provide further benefits. Therefore, we focus on examining the influence of the maximum distance to these additional samples. The results in Fig. 4 show that even our simple fusion of predicted probabilities generally improves performance, both with and without thresholding. The fusion of BEV features, on the other hand, shows no significant benefit. For 2.5% label utilisation we observe that increasing the range to above 20m is required to improve performance, whereas for 10% the maximum range is not as important. In further experiments, we will use 30m as it works well for both utilisation ratios. While the simple probability fusion strategy yields strong results, exploring more advanced fusion techniques is a promising avenue for future research.

F. Combining Components

Building on the above results, we further explore how these components interact in SSL for online mapping. Starting with the teacher-student setup as a *Core* we incrementally add components and evaluate their impact on performance. Here, we add strong augmentations to the student, *+Augs*, with Photometric, CutOut, and BEVDrop. Teacher fusion, *+Fusion*, is used with a maximum range of 30m. The Cosine feature similarity loss is incorporated under *+Featsim* with a weight of $w_{feat} = 0.25$. Additionally, a threshold of 0.6 is used without any temperature sharpening in *+Thr*, and hard pseudo-labeling is further added and denoted with *+Hard*.

The results in Tab. III demonstrate that combining components leads to further increased performance. Adding strong augmentations to the student yields a significant performance boost, as does further incorporating teacher fusion. Together these contribute to mIoU gains of 16.1 and 15.1 for 2.5% and

TABLE III: mIoU when incrementally adding SSL components.

Label Util.	Core	+Augs	+Fusion	+Featsim	+Thr.	+Hard
2.5%	12.1 \pm 0.6	25.5 \pm 0.7	28.2 \pm 0.7	29.0 \pm 0.6	29.4 \pm 0.3	29.3 \pm 1.1
10%	21.3 \pm 0.2	34.3 \pm 0.1	36.4 \pm 0.2	36.4 \pm 0.5	36.8 \pm 0.2	36.7 \pm 0.3

10% respectively. When combined with Fusion, feature similarity slightly improves performance for 2.5% labelled data, but has no impact for 10%. Finally, applying thresholding yields a modest improvement for both ratios, while using the hard pseudo-labels does not contribute further. These results underscore the importance of conducting ablation studies across different labelled data ratios, as the impact of various modules can vary depending on the amount of labelled data.

G. Varying Label Utilisation

We are also interested in how our proposed SSL method scales with varying amounts of labelled data. Using the parameters from Sec. IV-F, our proposed method includes strong augmentations, teacher fusion, Cosine feature similarity, and thresholding. Tab. IV displays performance when using both unlabelled and labelled data against using *only* the labelled data. Each setup is repeated three times with different data folds. As before, we report the mean and standard deviation; however, in this case, we select the best-performing model on the validation set and evaluate it on the test set. Besides conducting experiments on AV2 [45], we also use NuScenes [3], using the same hyperparameters except for learning rate and weight decay. As expected, performance decreases as the amount of labelled data is reduced. Here, we experiment using 100% of the data, corresponding to 700 sequences, down to only 18 sequences at 2.5% utilisation. Using the unlabelled data and our proposed setup yields significant performance gains across all labelled data utilisation ratios. In the lowest setting, relying solely on the labelled sequences results in poor performance, with mIoU dropping as low as 7.5 for AV2 and 5.6 for nuScenes. However, incorporating unlabelled data significantly boosts performance to 28.9 and 15.5 mIoU for the two datasets respectively. Using only 10% of the labels, the performance gap between using the unlabelled data and not is reduced from 29.6 mIoU to 3.5 mIoU on AV2, and from 12 mIoU to 3.4 mIoU on NuScenes.

TABLE IV: Test performance (mIoU) for multiple label utilisations for both Argoverse 2 (AV2) and NuScenes (NuSc).

	+Unblld Data	Label utilisation					
		2.5%	5%	10%	25%	50%	100%
AV2	✗	7.5 \pm 0.9	9.4 \pm 0.1	10.6 \pm 0.2	23.4 \pm 0.5	33.8 \pm 0.7	40.2 \pm 0.7
	✓	28.9\pm1.2	33.8\pm0.6	36.7\pm0.9	37.4\pm0.8	39.6\pm0.3	–
NuSc	✗	5.6 \pm 0.3	7.2 \pm 2.3	16.6 \pm 3.0	24.5 \pm 2.2	27.4 \pm 2.7	28.6 \pm 2.4
	✓	15.5\pm1.2	22.0\pm1.6	25.1\pm1.9	27.4\pm1.8	27.8\pm2.8	–

H. City Adaptation

We are interested in determining whether the proposed method can be used to adapt the model to a new city. To investigate this, we evaluate the model’s performance using the AV2 Far Extrapolation splits proposed by [27] and the

Boston to Singapore split used in [33] for NuScenes. For all runs, we use all labelled data from the source cities while gradually increasing the amount of unlabelled data from the target cities, ensuring that this data remains geographically disjoint from the test set. As reported in Tab. V, we find that, despite having no labelled data from the target city, we can significantly improve performance in that city by leveraging unlabelled data from it. In the AV2 dataset, our approach nearly matches the performance of a model trained using all target labels not included in the test set. *E.g.*, when adapting to Pittsburgh, the performance difference between using labelled data and our method is only 0.5 mIoU. However, it is noteworthy that the domain gap between the cities in AV2 is smaller since all cities are located in the United States. For NuScenes, the domain gap between Boston and Singapore is substantial, making it a more challenging problem. Yet our proposed method increases the mIoU from 11.1 to 17.0 using 100 unlabelled sequences from Singapore.

TABLE V: Performance (mIoU) for city adaptation for both Argoverse 2 and NuScenes when increasing amount of unlabelled data.

	Folds	# unlabelled target sequences					Using target labels
		0	25	50	100	200	
AV2	PIT-MIA \rightarrow Rest	33.6	34.4	35.5	37.5	37.2	38.9
	MIA-Rest \rightarrow PIT	36.3	38.7	40.0	40.2	40.7	41.2
	PIT-Rest \rightarrow Mia	34.5	36.1	37.5	37.8	38.5	40.2
NuSc	Boston \rightarrow Singapore	11.1	12.6	15.3	17.0	17.7	27.0

V. CONCLUSION

This paper draws inspiration from semi-supervised learning (SSL) techniques in other domains, demonstrating how to apply them to online mapping. For instance, we have shown that applying Photometric, CutOut, and BEV feature dropout augmentations to the student network significantly improves performance in a teacher-student setup. Further, we show that our proposed multi-step fusion for improving the teachers’ pseudo-labels yields an additional performance boost and that the Cosine similarity loss can help improve learning.

Combining the methods explored in this paper, performance can be significantly increased when also utilising unlabelled data for both Argoverse 2 and NuScenes compared to only using the labelled data. For instance, merely using 10% of the labels, the performance gap between using the unlabelled data and not is reduced from 29.6 mIoU to 3.5 mIoU on Argoverse 2, and from 12 mIoU to 3.4 mIoU on NuScenes. We have also shown that our method can be used for city adaptation, where we have labels for one city but not for the other. For example, when adapting from Boston to Singapore, performance is increased by 6.6 mIoU when unlabelled data from Singapore is included during training.

In summary, efficient use of both labelled and unlabelled data is crucial for advancing the field of online mapping. While we could not explore all existing SSL methods, this work takes a step toward understanding the strengths and weaknesses of core SSL methods in this context, aiming to inspire further research in this area. Future research could explore more rigorous teacher fusion over multiple samples or incorporate self-supervision tasks for further advancement.

Acknowledgements We want to express our sincere gratitude to Adam Tonderski, Georg Hess, William Ljungbergh, Carl Lindström, and Ji Lan for their continuous support and invaluable discussions. This work was partially supported by the Wallenberg AI, Autonomous Systems and Software Program (WASP) funded by the Knut and Alice Wallenberg Foundation. Computational resources were provided by the National Academic Infrastructure for Supercomputing in Sweden (NAISS) at [NSC Berzelius](#) and [C3SE Alvis](#) partially funded by the Swedish Research Council through grant agreement no. 2022-06725.

REFERENCES

- [1] David Berthelot, Nicholas Carlini, Ekin D Cubuk, Alex Kurakin, Kihyuk Sohn, Han Zhang, and Colin Raffel. Remixmatch: Semi-supervised learning with distribution alignment and augmentation anchoring. *arXiv preprint arXiv:1911.09785*, 2019.
- [2] David Berthelot, Nicholas Carlini, Ian Goodfellow, Nicolas Papernot, Avital Oliver, and Colin A Raffel. Mixmatch: A holistic approach to semi-supervised learning. *Advances in neural information processing systems*, 32, 2019.
- [3] Holger Caesar, Varun Bankiti, Alex H Lang, Sourabh Vora, Venice Erin Liong, Qiang Xu, Anush Krishnan, Yu Pan, Giancarlo Baldan, and Oscar Beijbom. nuscenes: A multimodal dataset for autonomous driving. In *IEEE Conference on Computer Vision and Pattern Recognition (CVPR)*, pages 11621–11631, 2020.
- [4] Nicolas Carion, Francisco Massa, Gabriel Synnaeve, Nicolas Usunier, Alexander Kirillov, and Sergey Zagoruyko. End-to-end object detection with transformers. In *European conference on computer vision*, pages 213–229. Springer, 2020.
- [5] Mathilde Caron, Hugo Touvron, Ishan Misra, Hervé Jégou, Julien Mairal, Piotr Bojanowski, and Armand Joulin. Emerging properties in self-supervised vision transformers. In *Proceedings of the IEEE/CVF international conference on computer vision*, pages 9650–9660, 2021.
- [6] Jiacheng Chen, Yuefan Wu, Jiaqi Tan, Hang Ma, and Yasutaka Furukawa. Maptracker: Tracking with strided memory fusion for consistent vector hd mapping. *arXiv preprint arXiv:2403.15951*, 2024.
- [7] Mu Chen, Zhedong Zheng, and Yi Yang. Transferring to real-world layouts: A depth-aware framework for scene adaptation, 2024.
- [8] Ting Chen, Simon Kornblith, Mohammad Norouzi, and Geoffrey Hinton. A simple framework for contrastive learning of visual representations. In *International conference on machine learning*, pages 1597–1607. PMLR, 2020.
- [9] Xinlei Chen and Kaiming He. Exploring simple siamese representation learning. In *Proceedings of the IEEE/CVF conference on computer vision and pattern recognition*, pages 15750–15758, 2021.
- [10] Ekin D Cubuk, Barret Zoph, Jonathon Shlens, and Quoc V Le. Randaugment: Practical automated data augmentation with a reduced search space. In *Proceedings of the IEEE/CVF conference on computer vision and pattern recognition workshops*, pages 702–703, 2020.
- [11] Terrance DeVries and Graham W Taylor. Improved regularization of convolutional neural networks with cutout. *arXiv preprint arXiv:1708.04552*, 2017.
- [12] Hao Dong, Xianjing Zhang, Jintao Xu, Rui Ai, Weihao Gu, Huimin Lu, Juho Kannala, and Xieyuanli Chen. Superfusion: Multilevel lidar-camera fusion for long-range hd map generation. In *Proceedings of the IEEE International Conference on Robotics and Automation (ICRA)*, 2023.
- [13] Geoff French, Samuli Laine, Timo Aila, Michal Mackiewicz, and Graham Finlayson. Semi-supervised semantic segmentation needs strong, varied perturbations. *The British Machine Vision Conference*, 2020.
- [14] Shuang Gao, Qiang Wang, and Yuxiang Sun. S2g2: Semi-supervised semantic bird-eye-view grid-map generation using a monocular camera for autonomous driving. *IEEE Robotics and Automation Letters*, 7(4):11974–11981, 2022.
- [15] Nikhil Gosala, Kürsat Petek, Paulo LJ Drews-Jr, Wolfram Burgard, and Abhinav Valada. Skyeye: Self-supervised bird’s-eye-view semantic mapping using monocular frontal view images. In *Proceedings of the IEEE/CVF Conference on Computer Vision and Pattern Recognition*, pages 14901–14910, 2023.
- [16] Nikhil Gosala, Kürsat Petek, B Ravi Kiran, Senthil Yogamani, Paulo Drews-Jr, Wolfram Burgard, and Abhinav Valada. Letsmap: Unsupervised representation learning for semantic bev mapping. *European Conference on Computer Cision (ECCV)*, 2024.
- [17] Chuan Guo, Geoff Pleiss, Yu Sun, and Kilian Q Weinberger. On calibration of modern neural networks. In *International conference on machine learning*, pages 1321–1330. PMLR, 2017.
- [18] Adam W Harley, Zhaoyuan Fang, Jie Li, Rares Ambrus, and Katerina Fragkiadaki. Simple-bev: What really matters for multi-sensor bev perception? In *2023 IEEE International Conference on Robotics and Automation (ICRA)*, pages 2759–2765. IEEE, 2023.
- [19] Kaiming He, Xinlei Chen, Saining Xie, Yanghao Li, Piotr Dollár, and Ross Girshick. Masked autoencoders are scalable vision learners. In *Proceedings of the IEEE/CVF conference on computer vision and pattern recognition*, pages 16000–16009, 2022.
- [20] Kaiming He, Xiangyu Zhang, Shaoqing Ren, and Jian Sun. Deep residual learning for image recognition. In *Proceedings of the IEEE conference on computer vision and pattern recognition*, pages 770–778, 2016.
- [21] Haruya Ishikawa, Takumi Iida, Yoshinori Konishi, and Yoshimitsu Aoki. Pct: Perspective cue training framework for multi-camera bev segmentation. *arXiv preprint arXiv:2403.12530*, 2024.
- [22] Dong-Hyun Lee et al. Pseudo-label: The simple and efficient semi-supervised learning method for deep neural networks. In *Workshop on challenges in representation learning, ICML*, volume 3, page 896. Atlanta, 2013.
- [23] Gang Li, Xiang Li, Yujie Wang, Yichao Wu, Ding Liang, and Shanshan Zhang. Pseco: Pseudo labeling and consistency training for semi-supervised object detection. In *European Conference on Computer Vision*, pages 457–472. Springer, 2022.
- [24] Qi Li, Yue Wang, Yilun Wang, and Hang Zhao. Hdmapnet: An online hd map construction and evaluation framework. In *2022 International Conference on Robotics and Automation (ICRA)*, pages 4628–4634. IEEE, 2022.
- [25] Bencheng Liao, Shaoyu Chen, Xinggang Wang, Tianheng Cheng, Qian Zhang, Wenyu Liu, and Chang Huang. MapTR: Structured modeling and learning for online vectorized HD map construction. In *The Eleventh International Conference on Learning Representations*, 2023.
- [26] Bencheng Liao, Shaoyu Chen, Yunchi Zhang, Bo Jiang, Qian Zhang, Wenyu Liu, Chang Huang, and Xinggang Wang. Maptrv2: An end-to-end framework for online vectorized hd map construction, 2023.
- [27] Adam Lilja, Junsheng Fu, Erik Stenborg, and Lars Hammarstrand. Localization is all you evaluate: Data leakage in online mapping datasets and how to fix it. In *Proceedings of the IEEE/CVF Conference on Computer Vision and Pattern Recognition*, pages 22150–22159, 2024.
- [28] Tsung-Yi Lin, Priya Goyal, Ross Girshick, Kaiming He, and Piotr Dollár. Focal loss for dense object detection. In *Proceedings of the IEEE international conference on computer vision*, pages 2980–2988, 2017.
- [29] Carl Lindström, Georg Hess, Adam Lilja, Maryam Fatemi, Lars Hammarstrand, Christoffer Petersson, and Lennart Svensson. Are nerf’s ready for autonomous driving? towards closing the real-to-simulation gap. In *Proceedings of the IEEE/CVF Conference on Computer Vision and Pattern Recognition*, pages 4461–4471, 2024.
- [30] Xiaolu Liu, Song Wang, Wentong Li, Ruizhi Yang, Junbo Chen, and Jianke Zhu. Mgmmap: Mask-guided learning for online vectorized hd map construction. In *Proceedings of the IEEE/CVF Conference on Computer Vision and Pattern Recognition*, pages 14812–14821, 2024.
- [31] Yicheng Liu, Tianyuan Yuan, Yue Wang, Yilun Wang, and Hang Zhao. Vectormapnet: End-to-end vectorized hd map learning. In *International Conference on Machine Learning*, pages 22352–22369. PMLR, 2023.
- [32] Yen-Cheng Liu, Chih-Yao Ma, Zijian He, Chia-Wen Kuo, Kan Chen, Peizhao Zhang, Bichen Wu, Zsolt Kira, and Peter Vajda. Unbiased teacher for semi-supervised object detection. *International Conference on Learning Representations (ICLR)*, 2021.
- [33] Yunze Man, Liangyan Gui, and Yu-Xiong Wang. Dualcross: Cross-modality cross-domain adaptation for monocular bev perception. In *2023 IEEE/RSJ International Conference on Intelligent Robots and Systems (IROS)*, pages 10910–10917. IEEE, 2023.
- [34] Lang Peng, Zhirong Chen, Zhangjie Fu, Pengpeng Liang, and Erkang Cheng. Bevsegformer: Bird’s eye view semantic segmentation from arbitrary camera rigs. In *Proceedings of the IEEE/CVF Winter Conference on Applications of Computer Vision (WACV)*, pages 5935–5943, January 2023.

- [35] Lang Peng, Zhirong Chen, Zhangjie Fu, Pengpeng Liang, and Erkang Cheng. Bevsegformer: Bird’s eye view semantic segmentation from arbitrary camera rigs. In *Proceedings of the IEEE/CVF Winter Conference on Applications of Computer Vision*, pages 5935–5943, 2023.
- [36] Jonah Philion and Sanja Fidler. Lift, splat, shoot: Encoding images from arbitrary camera rigs by implicitly unprojecting to 3d. In *Computer Vision—ECCV 2020: 16th European Conference, Glasgow, UK, August 23–28, 2020, Proceedings, Part XIV 16*, pages 194–210. Springer, 2020.
- [37] Kihyuk Sohn, David Berthelot, Nicholas Carlini, Zizhao Zhang, Han Zhang, Colin A Raffel, Ekin Dogus Cubuk, Alexey Kurakin, and Chun-Liang Li. Fixmatch: Simplifying semi-supervised learning with consistency and confidence. *Advances in neural information processing systems*, 33:596–608, 2020.
- [38] Carole H Sudre, Wenqi Li, Tom Vercauteren, Sebastien Ourselin, and M Jorge Cardoso. Generalised dice overlap as a deep learning loss function for highly unbalanced segmentations. In *Deep Learning in Medical Image Analysis and Multimodal Learning for Clinical Decision Support: Third International Workshop, DLMIA 2017, and 7th International Workshop, ML-CDS 2017, Held in Conjunction with MICCAI 2017, Québec City, QC, Canada, September 14, Proceedings 3*, pages 240–248. Springer, 2017.
- [39] Antti Tarvainen and Harri Valpola. Mean teachers are better role models: Weight-averaged consistency targets improve semi-supervised deep learning results. *Advances in neural information processing systems*, 30, 2017.
- [40] Wilhelm Tranheden, Viktor Olsson, Juliano Pinto, and Lennart Svensson. Dacs: Domain adaptation via cross-domain mixed sampling. In *Proceedings of the IEEE/CVF winter conference on applications of computer vision*, pages 1379–1389, 2021.
- [41] Vikas Verma, Kenji Kawaguchi, Alex Lamb, Juho Kannala, Arno Solin, Yoshua Bengio, and David Lopez-Paz. Interpolation consistency training for semi-supervised learning. *Neural Networks*, 145:90–106, 2022.
- [42] Erik Wallin, Lennart Svensson, Fredrik Kahl, and Lars Hammarstrand. Doublematch: Improving semi-supervised learning with self-supervision. In *2022 26th International Conference on Pattern Recognition (ICPR)*, pages 2871–2877. IEEE, 2022.
- [43] Xiao Wang, Daisuke Kihara, Jiebo Luo, and Guo-Jun Qi. Enact: A self-trained framework for semi-supervised and supervised learning with ensemble transformations. *IEEE Transactions on Image Processing*, 30:1639–1647, 2021.
- [44] Yidong Wang, Hao Chen, Qiang Heng, Wenxin Hou, Yue Fan, Zhen Wu, Jindong Wang, Marios Savvides, Takahiro Shinozaki, Bhiksha Raj, et al. Freematch: Self-adaptive thresholding for semi-supervised learning. *International Conference on Learning Representations (ICLR)*, 2023.
- [45] Benjamin Wilson, William Qi, Tanmay Agarwal, John Lambert, Jagjeet Singh, Siddhesh Khandelwal, Bowen Pan, Ratnesh Kumar, Andrew Hartnett, Jhony Kaesemodel Pontes, Deva Ramanan, Peter Carr, and James Hays. Argoverse 2: Next generation datasets for self-driving perception and forecasting. In *Proceedings of the Neural Information Processing Systems Track on Datasets and Benchmarks (NeurIPS Datasets and Benchmarks)*, 2021.
- [46] Enze Xie, Zhiding Yu, Daquan Zhou, Jonah Philion, Anima Anandkumar, Sanja Fidler, Ping Luo, and Jose M Alvarez. M²bev: Multi-camera joint 3d detection and segmentation with unified birds-eye view representation. *arXiv preprint arXiv:2204.05088*, 2022.
- [47] Mengde Xu, Zheng Zhang, Han Hu, Jianfeng Wang, Lijuan Wang, Fangyun Wei, Xiang Bai, and Zicheng Liu. End-to-end semi-supervised object detection with soft teacher. In *Proceedings of the IEEE/CVF international conference on computer vision*, pages 3060–3069, 2021.
- [48] Lihe Yang, Lei Qi, Litong Feng, Wayne Zhang, and Yinghuan Shi. Revisiting weak-to-strong consistency in semi-supervised semantic segmentation. In *Proceedings of the IEEE/CVF Conference on Computer Vision and Pattern Recognition*, pages 7236–7246, 2023.
- [49] Sangdoon Yun, Dongyoon Han, Seong Joon Oh, Sanghyuk Chun, Junsuk Choe, and Youngjoon Yoo. Cutmix: Regularization strategy to train strong classifiers with localizable features. In *Proceedings of the IEEE/CVF international conference on computer vision*, pages 6023–6032, 2019.
- [50] Xiaohua Zhai, Avital Oliver, Alexander Kolesnikov, and Lucas Beyer. S4l: Self-supervised semi-supervised learning. In *Proceedings of the IEEE/CVF International Conference on Computer Vision (ICCV)*, October 2019.
- [51] Bowen Zhang, Yidong Wang, Wenxin Hou, Hao Wu, Jindong Wang, Manabu Okumura, and Takahiro Shinozaki. Flexmatch: Boosting semi-supervised learning with curriculum pseudo labeling. *Advances in Neural Information Processing Systems*, 34:18408–18419, 2021.
- [52] Yunpeng Zhang, Zheng Zhu, Wenzhao Zheng, Junjie Huang, Guan Huang, Jie Zhou, and Jiwen Lu. Beverse: Unified perception and prediction in birds-eye-view for vision-centric autonomous driving. *arXiv preprint arXiv:2205.09743*, 2022.
- [53] Zhixin Zhang, Yiyuan Zhang, Xiaohan Ding, Fusheng Jin, and Xianguyu Yue. Online vectorized hd map construction using geometry. *arXiv preprint arXiv:2312.03341*, 2023.
- [54] Zhen Zhao, Lihe Yang, Sifan Long, Jimin Pi, Luping Zhou, and Jindong Wang. Augmentation matters: A simple-yet-effective approach to semi-supervised semantic segmentation. In *Proceedings of the IEEE/CVF conference on computer vision and pattern recognition*, pages 11350–11359, 2023.
- [55] Junyu Zhu, Lina Liu, Yu Tang, Feng Wen, Wanlong Li, and Yong Liu. Semi-supervised learning for visual bird’s eye view semantic segmentation. In *ICRA*, 2024.
- [56] Yang Zou, Zhiding Yu, Xiaofeng Liu, BVK Kumar, and Jinsong Wang. Confidence regularized self-training. In *Proceedings of the IEEE/CVF international conference on computer vision*, pages 5982–5991, 2019.